13th International Symposium on Turbulence and Shear Flow Phenomena (TSFP13)
Montreal, Canada, June 25–28, 2024

Towards a new roughness parametrization through the Effective Distribution function

Federica Bruno[1], Mauro De Marchis[2], and Stefano Leonardi[3]

[1]Department of Architecture and Engineering, University Kore of Enna, EN, Italy
[2]Department of Engineering, University of Palermo, Palermo, Italy.
[3]Department of Mechanical Engineering, University of Texas at Dallas, Richardson, TX, USA

1 Abstract

In a wide range of engineering applications, turbulent flows over rough surfaces are commonly encountered. Despite decades of research, accurately predicting drag and roughness function solely from surface geometrical parameters remains an unresolved issue. Various attempts have been made to identify combinations of these parameters that reliably correlate with surface drag. However, significant variability in results has been observed. It is hypothesized that not all roughness elements contribute equally to drag. Specifically, elements in the wake of larger ones may have minimal impact on drag, while isolated peaks can induce significant pressure drops compared to a uniformly distributed roughness with equivalent volume and frontal area. To test this hypothesis, simulations were conducted of turbulent flow over rough surfaces composed of triangular elements, varying their height distribution and spatial arrangement. Results indicate that geometries with identical effective slope, skewness, and kurtosis can exhibit distinct drag and roughness functions. A new geometrical parameter, the Effective Distribution, is introduced, showing strong correlation with drag within the range of variability considered in the study.

2 Introduction

Rough surfaces are encountered in a wide range of engineering and environmental applications. The flow in heat exchangers, the atmospheric boundary layer over urban areas, complex topography or vegetation and the leading edge erosion of turbine blades are just a few examples of the wide range of problems where roughness plays a key role. Roughness in general leads to a drop in system performance and a huge boost in the management costs. Hence, predicting the effect of rough walls on turbulence has become an important design prerequisite for practical applications. In the last decades, several studies have been carried out to understand the flows physics over corrugated walls, starting from the seminal work of Nikuradse Nikuradse (1993). Despite extensive efforts have been made by the scientific community, our knowledge cannot be considered sufficiently robust and universal yet. One of the first attempts to predict the main roughness effect was given by Hama (1954), introducing the correlation between a geometrical parameter, known as equivalent sand grain roughness k_s and the energy loss induced by the roughness. Hama (1954) observed that the main effect of the roughness is the downward shift of the mean velocity profile (scaled in inner units) in the log region, known as Roughness function ΔU^+ (hereafter, the superscript $^+$ denotes variables made non-dimensional with inner variables $u_\tau = (\tau_s/\rho)^{(0.5)}$ and ν/u_τ , where $u_\tau$is the friction velocity, τ_s is the wall stress, ρ the fluid density and ν the kinematic viscosity).

$$\Delta U^+ = \frac{1}{\kappa} ln(k_s^+) + B \tag{1}$$

where κ is the von K$\grave{a}$rm$\grave{a}$n constant, k_s^+=$k_s \cdot \nu/u_\tau$ and B is a constant. Unfortunately, k_s cannot be assigned a priori; it can be, in fact, determined once the mean velocity profile over the rough wall is known. Moreover, as pointed out by several authors (see among others Flack et al. (2020)), k_s isn't a physical measure of the corrugation. The prediction of the drag, as well as roughness function, based on geometrical features of the wall, has received extensive attention in the past and a variety of roughness correlations have been developed in literature (see among others Van Rij et al. (2002), Bons (2005), Napoli et al. (2008), Flack & Schultz (2010), Chan et al. (2015), Forooghi et al. (2017), Thakkar et al. (2017), Piomelli (2019), Chung et al. (2021). Several parameters were analyzed in the past, for instance the mean roughness height k^+, the peak-to-valley distance k^+_{pv}, the root mean square k^+_{rms} , the skewness S_k, the kurtosis K_s, the effective slope ES and the density parameter λ_s, using both experiments or numerical simulations over 2D or 3D roughness. Furthermore, some studies focused the attention on regular elements arranged over a flat plate (see among others Leonardi et al. (2003), Volino et al. (2011), Gatti et al. (2020), Modesti et al. (2021), Busse & Zhdanov (2022) for 2D elements and Orlandi & Leonardi (2008), Boppana et al. (2010), Hong et al. (2011), Busse & Jelly (2020) for 3D elements). Geometrical statistics, developed so far, correlate well with the drag of some particular type of roughness but lack universality and fail with other generic irregular walls. This calls for an effort to develop a universal correlation to predict roughness effects. In this study, Direct Numerical Simulations (*DNSs*) have been performed to reveal the influence of rough elements. A new parameter, called Effective Distribution *ED*, has been defined. The ED is based on a modified version of the known effective slope and the preliminary results show a good correlation with different roughness shape.Sect. 3 describes the numerical procedure adopted for DNS, Sect 4 highlights flow configurations, results are presented in 5 and conclusions are drawn in 6.

3 Numerical procedure

The non-dimensional Navier-Stokes and continuity equations for incompressible, neutrally stable flows can be expressed as

$$\frac{\partial U_i}{\partial t} + \frac{\partial U_i U_j}{\partial x_j} = -\frac{\partial P}{\partial x_i} + \frac{1}{Re}\frac{\partial^2 U_i}{\partial x_j^2} + \Pi\delta_{i1} \qquad (2)$$

$$\nabla \cdot \boldsymbol{U} = 0 \qquad (3)$$

where Re is the Reynolds number based on the bulk velocity (U_b $= 1/h\int_0^h U dy$), which is held constant in time, δ_{ij} is the Kronecker delta, U_i is the i-th component of the velocity vector, x_i is the i-th coordinate direction and P is the pressure per unit mass. The quantity Π is the pressure gradient which varies with time in order to keep constant the flow rate. The Navier-Stokes equations were discretized in an orthogonal coordinate system using the staggered central second-order finite difference approximation. The surface roughness was treated using the immersed boundary technique, which allows solution over complex geometries without the need for intensive body-fitted grids. This consisting of imposing $U_i = 0$ on the body surface, which does not necessary coincide with the grid. Full details about the immersed boundary method and the numerical schemes can be found in Orlandi & Leonardi (2006).

4 Flow configuration

Direct numerical simulations have been performed for an asymmetric fully developed turbulent channel flow with roughness on the bottom wall. The advantage of having an asymmetric channel is that the position of free shear is not forced to be at the centerline but it moves upward. The effective outer scale increases with respect to the half height of the channel, decreasing the k/h ratio as recommended by Jiménez (2004). Due to the difference of upper (smooth) and lower (rough) walls, here the total shear stress on the respective wall has been used (not the average between the two walls or the overall pressure gradient) for normalization in inner units. Periodic boundary conditions have been applied in streamwise (x) and spanwise (z) directions while no-slip condition has been imposed in wall-normal direction (y). The computational box in x, y, z

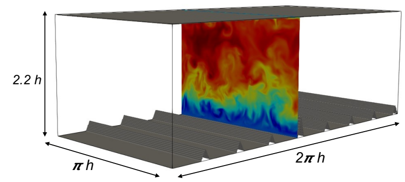

Figure 1: 3D computational domain for (one) the surfaces

direction is $6.4h \times 2.2h \times \pi h$ respectively; a sketch of one of the roughness cases here considered is shown in Figure 1). The computational domain has been discretized using $512 \times 256 \times 256$ grid points. The mesh is uniform in the streamwise and spanwise directions, with $\Delta x/h = 0.0125$ and $\Delta z/h = 0.0123$. On the other hand a non-uniform mesh has been used in the y direction. Specifically, in wall-normal direction the points are clustered near the wall within the cavity $\Delta y_{min}/h = 0.002$. The mesh increases toward the channel centerline, with $\Delta y_{max}/h = 0.03$. The Reynolds number is $Re = 4,300$ and corresponds to the friction Reynolds number $Re_\tau = 240$ when both walls are smooth. For a fixed pitch to height ratio $w/k = 4$, which is below the value for which transverse bars can be considered virtually isolated ($w/k = 7$, Leonardi et al. (2003)), two sets of simulations have been analyzed varying the roughness height k. The first set is made of 16 triangular transverse bars equally spaced in the streamwise direction $w/h = 0.4$. The baseline case (■ $A1_1$), has a constant roughness height $k/h = 0.1$. In the second set of simulations, we halved the number of triangular bars in streamwise direction but doubled the roughness height to $k/h = 0.2$ (■ case $A1_2$). The subscript indicates the roughness height. Other cases are considered as a modification of the baseline to highlight specific geometrical features, such as a protuberance above the roughness layer and the wake of larger elements affecting the downstream roughness. The height is slightly adjusted in each case to keep constant either the value of Effective Slope, kurtosis and skewness. In cases $B1_1$ (▲) and $B1_2$ (▲) we doubled the vertical size of one element; in cases $B2_1$ (▲), $B2_2$ (▲) and $B2_{2b}$ (▲) we removed the element immediately downstream the tallest one. The set of simulations labeled with C presents 2 taller triangles, with streamwise distances λ gradually increasing from $C1_1$ to $C4_1$ (●, ●, ●, ●) and from $C1_2$ to $C4_2$ (●, ●, ●, ●). The geometrical and flow properties are summarized in table 1.

5 Results and discussion

The effect of the roughness is to shift the mean velocity profile, with respect to that on a smooth wall, by an increment ΔU^+, referred to as the roughness function:

$$U^+ = \kappa^{-1}\ln y^+ + C - \Delta U^+ \qquad (4)$$

In figure 2 the total drag and the roughness function are plotted as function of the Effective Slope (ES), skewness and kurtosis

Marker	*Sketch*	*Case*	k/h	k_{max}/h	w/h	λ/h	ES	K_u	S_k	$D/\rho U_b^2$	ΔU^+
◆		Flat	0.00	0.0	0.0	0.0	0.00	0.00	0.00	0.12	0.3
■		$A1_1$	0.10	0.1	0.4	0.0	0.50	7.49	2.64	0.23	11.5
▲		$B1_1$	0.10	0.20	0.4	3.2	0.56	11.38	3.07	0.34	13.0
▲		$B2_1$	0.10	0.20	0.4	3.2	0.50	13.17	3.30	0.35	13.0
●		$C1_1$	0.09	0.18	0.4	0.4	0.56	11.61	3.13	0.28	12.2
●		$C2_1$	0.09	0.18	0.4	0.8	0.56	11.61	3.13	0.31	12.8
●		$C3_1$	0.09	0.18	0.4	1.2	0.56	11.61	3.13	0.37	13.5
●		$C4_1$	0.09	0.18	0.4	1.6	0.56	11.61	3.13	0.38	13.8
■		$A0$	0.20	0.0	6.4	0.0	0.06	7.49	2.64	0.23	11.0
■		$A1_2$	0.20	0.0	0.8	0.0	0.50	7.49	2.64	0.35	13.5
■		$A1_{2b}$	0.22	0.0	0.8	0.0	0.55	7.49	2.64	0.38	13.6
▲		$B1_2$	0.20	0.40	0.8	6.4	0.56	11.38	3.07	0.52	14.6
▲		$B2_2$	0.20	0.40	0.8	6.4	0.50	13.17	3.30	0.55	14.6
▲		$B2_{2b}$	0.23	0.46	0.8	6.4	0.58	13.17	3.30	0.68	15.5
●		$C1_2$	0.18	0.36	0.8	0.8	0.56	11.61	3.13	0.45	13.7
●		$C2_2$	0.18	0.36	0.8	1.6	0.56	11.61	3.13	0.49	14.2
●		$C3_2$	0.18	0.36	0.8	2.4	0.56	11.61	3.13	0.58	15.0
●		$C4_2$	0.18	0.36	0.8	3.2	0.56	11.61	3.13	0.60	15.0

Table 1: Geometrical and flow properties. k/h roughness height; k_{max}/h big element roughness height; w cavity width; λ distance between big elements; ES: effective slope; K_u Kurtosis; S_k Skewness; $D/\rho U_b^2$ total drag; ΔU^+ Roughness function.

(K_u). For the same ES, or K_u the drag and roughness function vary significantly, about $30-40\%$.

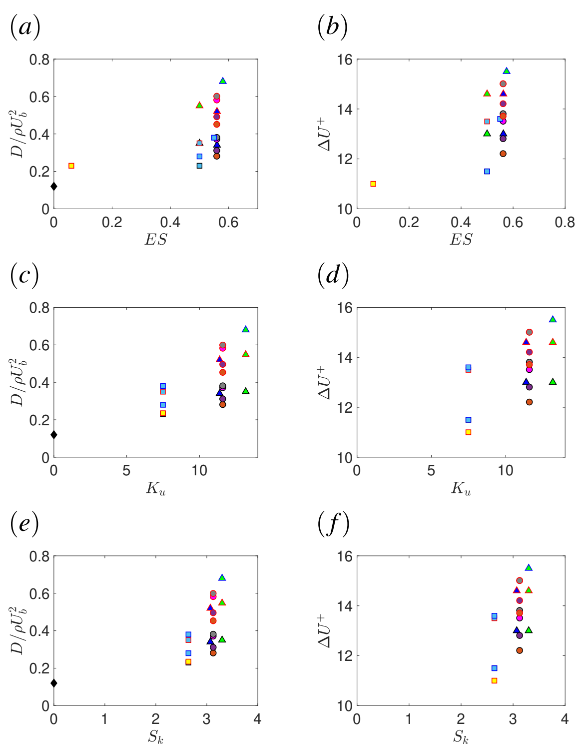

Figure 2: Roughness function and drag as function of the geometrical features of the rough wall (Effective slope, skewness and kurtosis). Symbols as in 1.

5.1 Inconsistency in geometrical parametrization

The flow structure and the pressure around the roughness elements have been analysed to assess why these geometrical features fail to depict the differences in drag and roughness function of the different cases we considered. Specifically, comparing case $A1_1$ (■ uniform triangles) and $B1_1$ cases, (▲ same as $A1_1$ with an element Δk higher), to a slight change of ES corresponds a major difference in drag. For uniform roughness, the cavities are filled with a recirculating flow (Fig.3a). The non dimensional form drag of each element is $P_d = 0.005$. On the other hand, in $B1_1$, the streamlines impinge on the tallest element (labeled "0" in Fig.3b for ease of identification) generating a strong stagnation point. The form drag is $P_d = 0.04$, about 8 times larger than that of uniform triangles. This shows how sensitive the drag is to pinnacles emerging outside the roughness layer, which, instead, is not accounted for in the ES, skewness and kurtosis. The form drag of the upstream triangle (labeled "-1") is slightly smaller because the streamlines are tilted upward by the taller element. The large recirculation closes on the second element downstream (labeled "2") at a distance of about $8k$. The pressure drag of the two roughness elements in the wake is very small and negative, meaning that the pressure on the leeward side is higher than that on the windward side. The drag of the other roughness elements is to a good approximation unaffected implying that a perturbation to the geometrical topography of the surface affects the flow slightly upstream (up to $4k$) and a bit more downstream ($8k$). The surface $B2_1$ is obtained by removing the triangle (labeled "1" in Fig.3b) downstream the highest roughness element. The mean streamlines are quite similar with those observed for the surface $B1_1$. In both cases, in fact, a main recirculation originated on the highest peak and closing about $8k$

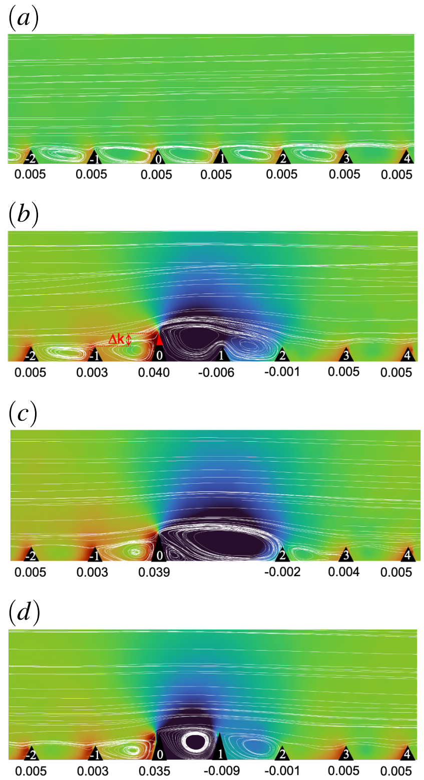

Figure 3: Streamlines superposed to color contours of pressure: a) $A1_1$ (■), b) $B1_1$ (▲), c) $B2_1$ (▲), d) $C1_1$ (●). The pressure drag of each triangle is indicated below them, i.e. $P_d(4) = 0.005$. Definition of Δk is included in the figure.

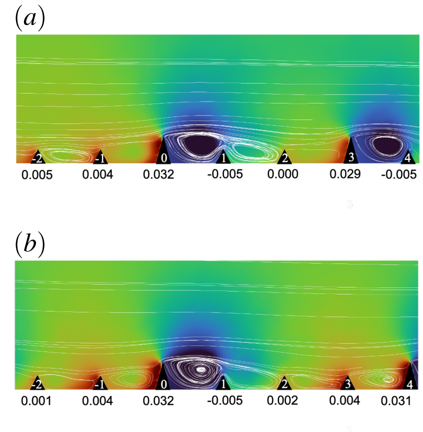

Figure 4: Streamlines superposed to color contours of pressure: a) $C3_1$ (●), b) $C4_1$ (●).

downstream (Fig.3c), can be observed. Furthermore, the overall drag and ΔU^+ are approximately the same as those of $B1_1$ despite variations of ES, S_k or K_u. This suggests that roughness elements located in the wake region of higher elements must be weighted differently in the geometrical statistics of the surface. Adding a second taller roughness element to $B1_1$, immediately downstream (labeled "1" in Fig.3d), surface $C1_1$, increases the mean surface height, as well as the higher moments statistics, but reduces the drag (and roughness function) instead of increasing it. The wake of the first higher pinnacle shields the second. The recirculation shrinks compared to $B1_1$ and $B1_2$, filling the cavity formed by the two higher triangles (elements "0" and "1" of Fig.3d).
Increasing the distance between the two highest pinnacles (cases $C3_1$ ● and $C4_1$ ●, Fig.4a,b), leads to an increase of drag and ΔU^+ because the streamlines tend to reattach on the lower array of triangles with a consequent increase of pressure drag on the large element. These results suggest that the position of the roughness elements affects the flow physics and the drag despite the geometrical features are the same. A single pinnacle much higher than the others have a major effect on the flow. Its contribution is not proportional to the wet area, or exposed area to the flow; it is much higher if the upstream elements are smaller. It could be interpreted mathematically into a geometry height gradient, which was partially taken into account by the ES. However, cases $C1_1 - C4_1$ highlight also how it is important the presence of other tall roughness elements upstream, and their wake. The distance λ between two consecutive highest peaks is a key parameter to determine the influence of roughness on turbulent flow.

5.2 Effective Distribution

The analysis of section 5.1 showed that any parametrization based on geometrical features of the walls needs to be consistent with the following:

- pinnacles emerging above the roughness layer produce a wake (Fig.3a). The roughness elements in the wake have a negligible contribution to the drag. As a consequence, the geometrical quantities used to parameterize the roughness should be filtered by the contribution of those elements in the wake length.
- the contribution to the drag of each roughness element depends on its size, distance from previous elements (figure 3b).

A new geometrical parametrization, Effective Distribution, is here proposed as a modification of the Effective Slope introduced by Napoli et al. (2008):

$$ED = ES - \sum_{i=1}^{n} \alpha_i \cdot ES_i + \sum_{i=1}^{m} \beta_i \cdot ES_{\Delta ki} + \sum_{i=1}^{s} \frac{lx_{i,flat} \cdot k}{Lx_{flat} \cdot \delta k} \qquad (5)$$

It is obtained from the original ES definition, by subtracting the contribution of roughness elements located in the wake region and adding the contribution of pinnacles above the crest plane. For all test cases analyzed, the *wake* was verified to be 8 time k_{max}. This result is consistent with previous experiments and

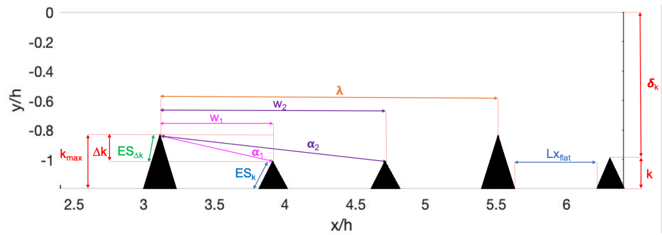

Figure 5: Effective Distribution

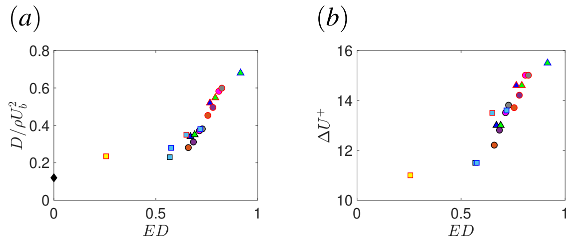

Figure 6: Roughness correlations: (a) Effective Slope (Napoli et al. (2008); (b) Effective Distribution.

numerical simulations in literature where it was observed that the cavity width w to roughness height k ratio achieve a critical value in the range $w/k \approx 7-8$. The coefficients α is the distance between each roughness element and the pinnacles, $\alpha = \frac{\Delta k_j}{w_i}$, where, Δk_j is the j-*th* roughness peak over the crest plane, whereas w_i is the distance between the i-*th* element from the j-*th* pinnacle. In Figure 5 a sketch of these distances is depicted. In addition, if the surface is characterized by more than one peak higher then the surrounding elements, the distance between two subsequent pinnacles, "λ," has to be considered. When $\lambda < 8k_{max}$, (recall that $8k_{max}$ is an approximation of the wake length), the downstream pinnacle is in the wake region of the upstream pinnacle. This means that the flow around the downstream pinnacle will be affected by the wake of the upstream pinnacle, which can result in a reduced contribution to the overall drag. To account for this effect, a coefficient β is introduced, which scales the contribution of the downstream pinnacle to the overall drag. When $\lambda < wake$, β is less than 1 to reflect the reduced contribution of the downstream pinnacle. As λ increases and the downstream pinnacle moves out of the wake region, β increases as well, until it reaches a constant value of 1 when λ is greater than the wake width. This indicates that both pinnacles have the same contribution to the overall drag and can be treated as isolated peaks. The ES does not provide information about the distance between one element and another, as in the case of a flat section where $ES = 0$. As observed by Leonardi et al. (2003), the velocity profile is strongly influenced by the flat region downstream of each element. The last term of the equation 5 was introduced to account for it.

Figure 6 shows the correlation between the Effective Distribution and the total drag or roughness function based on the above considerations. The correlation between ED and the drag significantly improves with respect to the Effective Slope, plotted in figures 2 and 6. This result suggests how the new geometrical parameter takes into account various geometrical features which effect the turbulent flows, such as the peaks above mean roughness, the wake region induced by the highest elements and the distance between two consecutive elements.

6 Conclusions

DNSs have been performed to analyze a set of 2D rough surfaces using triangle-shaped elements. One of the main challenges of the last decade was the prediction of drag and roughness function based on surface topography, which requires a parametrization. Therefore, seven rough walls with different shapes but similar effective slope, skewness, and kurtosis have been investigated. The study found that for most of the data, different shapes with the same geometrical quantities can result in different drag and roughness functions. To address this issue, a new geometrical parameter called Effective Distribution (ED) was introduced. The ED is a geometrical parameter that accounts for the physical behavior of fluid around roughness elements. It is calculated based on two hypotheses. First, elements with a larger roughness height than the roughness thickness produce a wake that influences the following corrugations, making negligible their contribution to the drag. Therefore, the geometrical statistics should be filtered by the contribution of those elements in the wake length or weighted differently. Secondly, rough elements have lesser or greater contributions based on their size and pattern. To validate these hypotheses, all test cases were analyzed, and the pressure distribution around the roughness elements were investigated. The results showed that roughness elements in the wake of trailing pinnacles do not affect the flow and give different contributions to the total drag. In fact, the triangles above the roughness base-layer have a larger contribution to the drag than the crest plane. The Effective Distribution has been calculated as a modification to the Effective Slope by subtracting the contribution of roughness elements located in the wake region and adding the contribution of pinnacles above the crest plane. The distance between each roughness element and the pinnacles is taken into account. Additionally, if the surface is characterized by more than one pinnacle, their distance has to be considered. Overall, the Effective Distribution provides a representative geometrical parameter of the entire roughness configuration, taking into account the peaks above the mean roughness, the wake region induced by the highest elements, and the distance between two consecutive elements. In this study, the Effective Distribution (ED) has shown to improve the correlation between roughness-related parameters such as total drag, drag coefficient, and roughness function. The Effective Slope showed a vertical alignment for most of the data, meaning that for a given Effective Slope value, there is a large variation in terms of drag and roughness function. This suggests that the Effective Slope alone may not fully capture the impact of geometrical features on turbulent flows. In contrast, the Effective Distribution improved the correlation with the drag by increasing the roughness-related value as the ED rises. This indicates that the ED takes into account various geometrical features that affect turbulent flows, such as peaks above mean roughness, wake regions induced by the highest elements, and the distance between two consecutive elements. Overall, the use of the Effective Distribution has improved the correlation between different parameters, but further analysis may be required to better understand the variation observed for the Effective Slope correlations.

References

Bons, J 2005 A critical assessment of reynolds analogy for turbine flows. J. Heat Transfer **127** (5), 472–485.

Boppana, VBL, Xie, Zheng-Tong & Castro, Ian P 2010 Large-eddy simulation of dispersion from surface sources in arrays of obstacles. Boundary-layer meteorology **135** (3), 433–454.

Busse, Angela & Jelly, Thomas O 2020 Influence of surface anisotropy on turbulent flow over irregular roughness. Flow, Turbulence and Combustion **104** (2), 331–354.

Busse, Angela & Zhdanov, Oleksandr 2022 Direct numerical simulations of turbulent channel flow over ratchet roughness. Flow, Turbulence and Combustion **109** (4), 1195–1213.

Chan, L, MacDonald, M, Chung, D, Hutchins, N & Ooi, A 2015 A systematic investigation of roughness height and wavelength in turbulent pipe flow in the transitionally rough regime. Journal of Fluid Mechanics **771**, 743–777.

Chung, Daniel, Hutchins, Nicholas, Schultz, Michael P & Flack, Karen A 2021 Predicting the drag of rough surfaces. Annual Review of Fluid Mechanics **53**, 439–471.

Flack, Karen A & Schultz, Michael P 2010 Review of hydraulic roughness scales in the fully rough regime. Journal of Fluids Engineering **132** (4).

Flack, Karen A, Schultz, Michael P & Volino, Ralph J 2020 The effect of a systematic change in surface roughness skewness on turbulence and drag. International Journal of Heat and Fluid Flow **85**, 108669.

Forooghi, Pourya, Stroh, Alexander, Magagnato, Franco, Jakirlić, Suad & Frohnapfel, Bettina 2017 Toward a universal roughness correlation. Journal of Fluids Engineering **139** (12).

Gatti, Davide, von Deyn, Lars, Forooghi, Pourya & Frohnapfel, Bettina 2020 Do riblets exhibit fully rough behaviour? Experiments in Fluids **61** (3), 1–6.

Hama, Francis R 1954 Boundary layer characteristics for smooth and rough surfaces. Trans. Soc. Nav. Arch. Marine Engrs. **62**, 333–358.

Hong, Jiarong, Katz, Joseph & Schultz, Michael P 2011 Near-wall turbulence statistics and flow structures over three-dimensional roughness in a turbulent channel flow. Journal of Fluid Mechanics **667**, 1–37.

Jiménez, Javier 2004 Turbulent flows over rough walls. Annu. Rev. Fluid Mech. **36**, 173–196.

Leonardi, S, Orlandi, Paolo, Smalley, RJ, Djenidi, L & Antonia, RA 2003 Direct numerical simulations of turbulent channel flow with transverse square bars on one wall. Journal of Fluid Mechanics **491**, 229–238.

Modesti, Davide, Endrikat, Sebastian, Hutchins, Nicholas & Chung, Daniel 2021 Dispersive stresses in turbulent flow over riblets. Journal of Fluid Mechanics **917**.

Napoli, E, Armenio, Vincenzo & De Marchis, M 2008 The effect of the slope of irregularly distributed roughness elements on turbulent wall-bounded flows. Journal of Fluid Mechanics **613**, 385–394.

Nikuradse, Johann 1993 Laws of flow in rough pipes.

Orlandi, Paolo & Leonardi, Stefano 2006 Dns of turbulent channel flows with two-and three-dimensional roughness. Journal of Turbulence (7), N73.

Orlandi, P & Leonardi, S 2008 Direct numerical simulation of three-dimensional turbulent rough channels: parameterization and flow physics. Journal of Fluid Mechanics **606**, 399–415.

Piomelli, Ugo 2019 Recent advances in the numerical simulation of rough-wall boundary layers. Physics and Chemistry of the Earth, Parts A/B/C **113**, 63–72.

Thakkar, Manan, Busse, Angela & Sandham, Neil 2017 Surface correlations of hydrodynamic drag for transitionally rough engineering surfaces. Journal of Turbulence **18** (2), 138–169.

Van Rij, Jennifer A, Belnap, BJ & Ligrani, PM 2002 Analysis and experiments on three-dimensional, irregular surface roughness. J. Fluids Eng. **124** (3), 671–677.

Volino, Ralph J, Schultz, Michael P & Flack, Karen A 2011 Turbulence structure in boundary layers over periodic two-and three-dimensional roughness. Journal of Fluid Mechanics **676**, 172–190.